Header will be provided by the publisher

Probing Floquet modes in a time periodic system with time defects using Faraday instability

GUILLAUME D'HARDEMARE[1], ANTONIN EDDI[2] AND EMMANUEL FORT [1(a)]

[1] *Institut Langevin, ESPCI Paris, CNRS, PSL University, 1 rue Jussieu, F-75005 Paris, France.*
[2] *PMMH, CNRS, ESPCI Paris, Université PSL, Sorbonne Université, Université de Paris, F-75005, Paris, France.*

received and accepted dates provided by the publisher
other relevant dates provided by the publisher

PACS 47.35.-i – Hydrodynamic waves
PACS 47.20.-k – Flow instabilities
PACS 03.65.Vf – Phases: geometric; dynamic or topological

Abstract – Time crystals are systems whose properties are periodically modulated in time. Among these, Floquet time crystals exhibit momentum gaps in their band structures, analogous to energy gaps in spatial crystals. Recently, time defects with a π-shift in the time modulation have been introduced theoretically as temporal analogues of spatial topological defects associated with localized edge modes. Here we perform experiments in a time periodic system using Faraday instability, a parametric excitation of a liquid bath by vertical shaking. Although time defects also trigger an exponentially decaying wave, we show that the analogy does not hold due to temporal causality and lack of energy conservation. However, these time defects provide an original way to explore momentum gaps and reveal their overdamped modes.

Introduction. – A new research area was stimulated by Frank Wilczek in 2012 who postulated by analogy to the spontaneous breaking of spatial invariance in a crystal that periodic time structures could emerge spontaneously in classical or quantum systems[1,2]. It turned out that this was possible for periodically driven systems to spontaneously self-organize and start evolving with a period different from the driving period. This has led to intensive theoretical and experimental developments on so-called discrete or Floquet time crystal[3–7]. Quantum Floquet time crystals have been implemented only recently in various quantum systems[8–14]. However, their classical counterparts have been known for quite a long time in astronomy[15], optics[16], mechanics[17,18] or fluid dynamics[19]. The first recorded demonstration of such a periodically driven system appears to have been that of Faraday instability in 1831[19]. The surface of a liquid bath submitted to a vertical sinusoidal shaking becomes unstable above a given acceleration threshold. Experiments with Faraday instability offer a great versatility and open a unique platform to investigate a large variety of condensed matter phenomena in the time domain beyond the self-organization and the breaking of time translation symmetry[20] like Anderson and many-body localization[21,22] or quasi-crystals[23]. Note that in the present paper, the term "time crystal" refers to a time symmetry breaking of the system whose dynamics responds at a sub-harmonic of the parametric driving frequency. It does not hold all the properties associated to quantum time crystal.

Very recently, it has been proposed to introduce topological concepts in the time domain[24,25]. The theoretical proposals in quantum time crystals[24] and in photonic time crystals[25] consisted in driving a system resonantly so that the emerging crystalline structure in time possess a symmetry protected topological phase. For spatial crystals, topologically protected edge states can be achieved by cascading two crystals with a topological defect which introduce a localized π-shift in the crystal periodicity (see Fig. 1a)[26]. The temporal analog could thus be obtained by introducing a similar π-shift defect in the time modulation, in which case localized exponentially decaying oscillations would be a signature of topological edge modes.

Here, we study experimentally this π-shift time defect in a time periodic system using Faraday instability. The paper is organized as follow: we first introduce Faraday instability with the framework of a time crystal. We then present the experimental set-up and give evidence of exponentially decaying localized mode. We then discuss what the differences with their spatial analogs are and how these modes are related to Floquet modes rather than localized topological edge modes. Finally, we show that these time defects offer an original way to investigate the Floquet modes and characterize the concealed overdamped modes.

Faraday instability as a time crystal. – The Faraday instability is observed when a liquid bath is vertically shaken above a given acceleration threshold. The surface then deforms

[(a)]E-mail: emmanuel.fort@espci.fr

into a standing wave pattern which oscillates at half the excitation frequency[27]. When considering the liquid in the moving frame, the vertical acceleration of the bath is formally equivalent to a periodic modulation of gravity around its standard value. As it depends on gravity, the dispersion relation and thus the speed of the waves also undergo a periodic modulation.

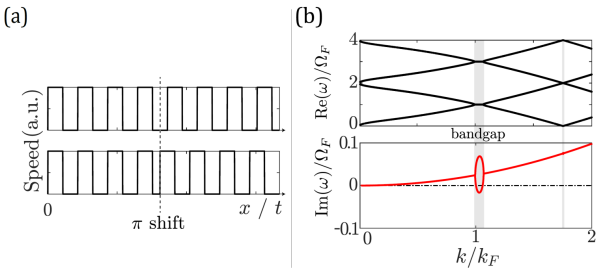

Fig. 1: (Colour on-line) a) Schematics of a time (t) or spatial (x) crystal showing a periodic modulation of the wave speed with time or in space respectively (top). Time or spatial defect in the form of a π-shift in the modulation (bottom) introduced between two time or space crystals respectively. b) Dispersion relation of the Faraday instability. Real part $\mathrm{Re}(\omega)/\Omega_F$ (top) and imaginary part $\mathrm{Im}(\omega)/\Omega_F$ (bottom) of the angular frequency ω normalized by the Faraday angular frequency Ω_F as a function of normalized wavenumber k/k_F, k_F being the Faraday wavenumber. The vertical gray bands are the vertical k-gaps. The small parabolic variation corresponds to the viscous damping. Within the k-gap, two solutions appear, overdamped or underdamped compared to the viscous damping. For sufficiently strong forcing, $\mathrm{Im}(\omega)$ becomes negative, resulting in exponential amplification of the signal.

Even though there is no equivalent of the speed of light for water waves, this is akin to having a medium where the refractive index varies periodically in time. The Faraday instability has mostly been studied as a hydrodynamic instability in the stationary regime. We propose to revisit this parametric instability within the framework of Floquet time crystals.

For an inviscid fluid in a bath submitted to vertical acceleration $a_0\cos(2\Omega_F t)$, the modes are given by a Mathieu equation[28]. The free surface elevation $\xi(\mathbf{r},t)$ at position $\mathbf{r}$ and time t can be decomposed in Fourier modes $\hat{\xi}(\mathbf{k},t)$ of wavevector $\mathbf{k}$ following

$$\frac{\partial^2\hat{\xi}(\mathbf{k},t)}{\partial t^2} + \omega_0^2(\boldsymbol{k})\hat{\xi}(\mathbf{k},t) = -a_0 k\cos(2\Omega_F t)\hat{\xi}(\mathbf{k},t) \qquad (1)$$

with $\omega_0(\mathrm{k})$ being the angular frequency given by the dispersion relation for gravity-capillary waves and k, the wavenumber. This equation describes the modes in a medium with a gravity modulation which induces a speed modulation[29,30].

The solutions of the Mathieu equation are given by the Bloch-Floquet theorem $\hat{\xi}(\mathbf{k},t) = e^{i\omega t}\sum_{n\in\mathbb{Z}} c_n(k)e^{in2\Omega_F t}$. In a fluid with a small viscosity ν, a damping term $-2\gamma\partial\hat{\xi}/\partial t$ should be added to the Mathieu equation, γ being the damping satisfying $\gamma = 2\nu k^2$. By a change of variables this new equation can also be rewritten as a damped-free Mathieu equation[31]. Figure 1b shows a typical dispersion curve obtained with a small viscosity. The upper panel shows the real part $\mathrm{Re}(\omega)$ of the angular frequency as a function of the normalized wavenumber k/k_F. We first note that in a similar fashion to spatial crystals, the periodicity of the medium (here in time), leads to a folding of the dispersion relation. For sufficiently strong potentials, a gap forms in the structure, which we highlighted in grey. These k-gaps are the equivalent of the energy bandgaps which appear in the band structure of spatial crystals. Whereas conservation of energy in spatial crystals implies that waves injected within the bandgap are bound to decay exponentially, no such restriction exists for temporal crystals in which energy is injected periodically. The lower panel of Figure 1b shows the imaginary part, $\mathrm{Im}(\omega)$ of the angular frequency as a function of the normalized wavenumber k/k_F. Outside of the bandgap the curve is given by viscous damping in the liquid. Within the k-gap, however, two solutions exist, respectively over and under damped with respect to the bath at rest (viscous damping). For sufficient forcing, a region appears with $\mathrm{Im}(\omega) < 0$, that is a region where an exponentially growing solution exists. Above this threshold, the Faraday instability is observed and a standing wave at half the excitation frequency appears. The transient growth of the standing wave pattern directly results from the exponential amplification of waves initially present in the noise. The corresponding mode with $\mathrm{Im}(\omega) > 0$ is overdamped and remains hidden. The two standing wave solutions have their phase locked on the parametric excitation and are in quadrature. Each standing wave can be described as the result of the interference of two counter-propagating Floquet modes with a relative phase which depends on their position in the k-gap.

The Faraday instability can therefore be interpreted as a medium in which the speed of the waves is modulated in time. When a propagating wave penetrates such a medium it generates a counter-propagating wave which can be considered as a time reversed (or phase-conjugated) wave together with a wave co-propagating with the initial wave[29,30]. In terms of time crystal, the two waves produced can be interpreted respectively as a time reflected wave and a time transmitted wave. Their characteristics are given by the time analog of Fresnel relations in optics[32].

Experimental Setup. – We now focus on an implementation of a 1D time crystal based on Faraday instability. Figure 2a shows the experimental setup. It consists in a 1D wave cavity. A glass tank of 40 mm depth, 200 mm length and 10 mm wide is placed on a vibrating shaker to perform sinusoidal vertical oscillations with a peak acceleration a_0 and an angular frequency $2\Omega_F$. Two horizontal T-shaped plastic strips (ii) pin the fluid contact line. One of the strip is mounted on a translation stage to tune the cavity length L. Note that the translation stage is mounted on the shaker to synchronize its vertical motion to that of the cavity. The tank is filled up with deionized water approximately 1 mm above the tank edges (iii). The Faraday waves are excited at half the forcing frequency $\Omega_F/2\pi$. Their associated wavelength λ_F is given by

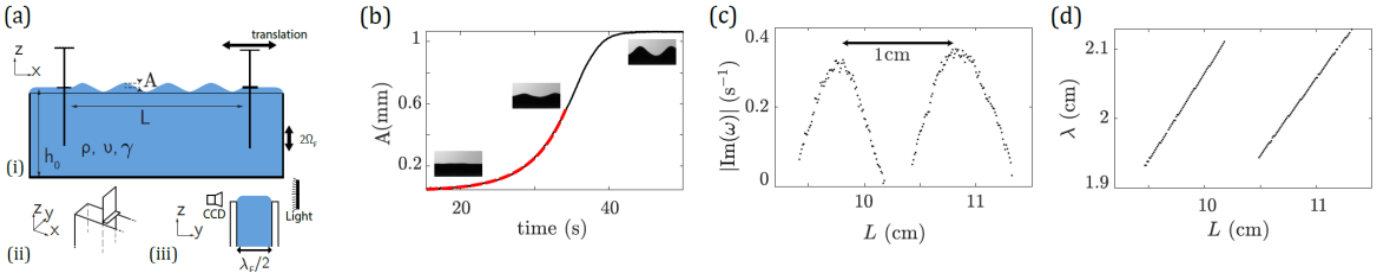

the capillary-gravity dispersion of water waves. To ensure the excitation of the transverse mode, we choose λ_F equal to twice the width of the cavity, which gives $\Omega_F/2\pi = 11.6$ Hz. Side-view movies of the water surface are recorded using a camera

Fig. 2: (Colour on-line) a) Experimental setup: a water tank is placed on a shaker (i). The width of the cavity is set to $\lambda_F/2 \sim 1$ cm. (ii) Schematics detailing the boundary conditions at the end of the cavity. The meniscus is pinned by the hovering plastic strip aligned along the y axis. (iii) Side view showing the meniscus pinned along the x axis. b) Typical evolution of the wave amplitude upon sufficient shaking of the bath. Exponential fit up to the inflection point (red dashed curve). Insets: snapshots of the water profile at various times. c) Growth rate of the waves $\mathrm{Im}(\omega)$ and d) mode wavelength λ in the cavity as a function of the cavity size L. c) and d) show results from the same experiment with forcing frequency equal to $2\Omega_F$.

at 464 fps under back-illumination condition with a resolution of 40 µm/px. The wave profile is retrieved with a subpixel precision using fine-tuned edge detection algorithms. The amplitude of the Faraday waves $A(t)$ is measured at the position of an anti-node.

Upon turning on the vibration of the bath above threshold at $t = 0$, the instability sets in and the waves begin to grow before reaching a saturation (Figure 2b). Insets show snapshots of the water surface at the different times (stretched in the vertical direction by a factor 4 for clarity). The red dashed line shows the good agreement of the experimental growth of the wave with an exponential fit up to the inflection point before a nonlinear saturation occurs and a plateau is reached. This gives the growth rate of the unstable Floquet mode which corresponds to the imaginary part of the Floquet exponent $\mathrm{Im}(\omega)$.

The evolution of $\mathrm{Im}(\omega)$ and the wavelength λ with the length of the cavity L are measured from the wave profiles (λ is measured in the stationary regime, for $t > 30$ s). The growth rates (Fig. 2c) exhibit peaks separated by $\lambda_F/2$ which correspond to the matching between k-gap mode and a resonant mode of the cavity with $\lambda = 2L_{\mathrm{eff}}/n$, n being the mode number and L_{eff} the effective cavity length taking into account the boundary conditions. Varying the cavity length results in scanning the k-gap associated to the Faraday instability (fig. 2d). The curve of the growth rate thus corresponds to a periodic scanning of the k-gap with maxima satisfying $L_{\mathrm{eff}} = n\lambda_F/2$.

Time defects. – We introduce a defect in the time crystal by suddenly π-shifting the excitation phase which amounts to concatenating two time crystals with opposite phase (Fig. 1b). A first time crystal starts at $t = 0$ with acceleration a_0 for 45 s. The end of the first crystal is immediately followed by the beginning of a second π-shifted time crystal. Figure 3a and 3b show the theoretical signal sent to the shaker and the experimental response respectively. The phase shift induces small perturbations which last approximately two periods. Figure 3c shows the evolution of the amplitude of the waves (See supplementary movie). Above the Faraday threshold, standing waves grow on the surface and reach a constant value due to a nonlinear hydrodynamic saturation (see Fig. 2b). At the interface between the two time crystals we observe a sudden decrease of the wave amplitude before the waves start to grow again to reach a saturation value. The initial standing mode associated with the first time crystal is in quadrature with the one associated with the second crystal. This enables the tracking of the decay of the envelope of the first mode (red solid line) together with that of the growing second mode (blue solid line). The effect of the time interface between the two periodic crystals is thus to permute the amplified and the overdamped modes of the two π-shifted crystals. Neglecting saturation effects, the waves initially present in the time crystals are thus exponentially decreasing away from the time interface in a similar way as spatial topological edge modes do from a spatial topological interface.

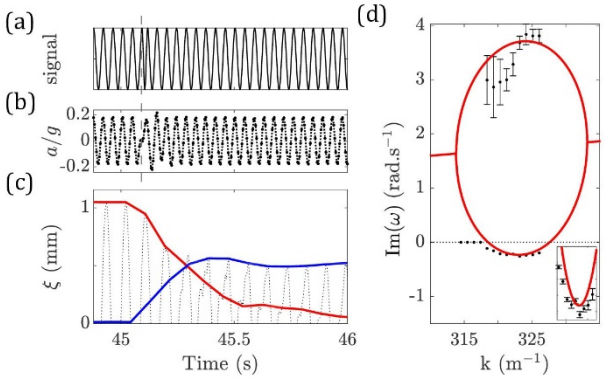

Fig. 3: (Colour on-line) a) Theoretical time signal sent to the shaker showing a π-phase shift at approximately t = 45 s. b) Measurement of corresponding tank acceleration. c) Positive half of the evolution of the surface elevation at the location of an anti-node (dotted line). Envelope of the surface elevation at the phase of the initially amplified mode (solid red line). Evolution of the envelope of the quadrature mode (solid blue line, see supplementary movie). d) Measurement of growth rates (bottom circle) from the exponential fit (see Fig. 2b) and the decay rates from the decay of the red curve (c). The red curves gives the result of the computation based on a damped Mathieu equation using experimental values of the viscosity deduced from Fig. 4 (inset: zoom on the lower part of the curve).

Probing the overdamped modes. – The two states associated to the two Floquet exponents within the k-gap correspond to two standing modes in quadrature, their role being exchanged at the interface. This enables the measurement of both

Floquet exponents from the measurement of the exponential decay and growth at the interface (see Fig. 3c). These exponents can be measured along the entire k-gap by tuning the size of the cavity (Black dots Fig. 3d and inset). The red line is the theoretical curve of the complex k-gap obtained from the damped Mathieu equation with no fitting parameter and an effective viscosity measured experimentally from Fig. 4 (see below). There is a very good agreement between the experimental results and the theoretical model.

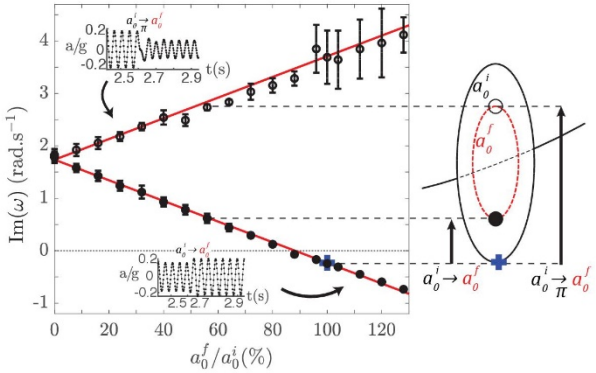

Fig. 4: (Colour on-line) Measured Floquet exponents $\mathrm{Im}(\omega)$ of the amplified and overdamped modes using the interface between two time crystals for a cavity set at the Faraday resonance. Principle (right): the system is prepared in an initial state with acceleration a_0^i (blue cross in the dispersion curves of the k-gap - black solid line). At the time interface, it undergoes a sudden change from a_0^i to a_0^f changing $\mathrm{Im}(\omega)$ (dashed red lines). Depending on the presence of a π-phase shift two transitions can be measured. The system jumps to either the solid black dot (no π-shift) or the hollow black dot (π-shift). Knowing the initial growth rate, we compute the values for each situation. The red lines (left) are theoretical computation from the damped Mathieu equation using the experimental values for the effective viscosity obtained at $a_0^f = 0$.

The π-shift defect enables waves associated to the amplified Floquet exponent to jump to the overdamped mode, i.e. the upper positive part of $\mathrm{Im}(\omega)$ which is otherwise hidden by the Faraday instability. In the following, we take advantage of this transition and more generally of the interface between two time crystals to explore the Floquet exponents in the k-gap. The cavity is tuned so that one of its resonant mode coincides with the Faraday wavenumber (middle of the k-gap). The first and second time crystals have different accelerations a_0^i and a_0^f respectively and the time interface may or may not contain a π-shift defect. Figure 4 (right) shows how the exponents of the complex dispersion relation $\mathrm{Im}(\omega)$ are measured. The initial state is given by the waves amplified by the Floquet exponent of the first time crystal (blue cross of the black solid lines). The second time crystal is associated to a different opening of the k-gap, in the example $a_0^f < a_0^i$ which results in a smaller opening (dashed red lines). After the time interface, the measured transition corresponds to different a final state depending on the presence of a π-shift defect (empty black circle) or not (full black circle). Figure 4 (left) shows the Floquet exponents measured for $a_0^i = 1.78\ \mathrm{m^2.s^{-1}}$ as a function of a_0^f/a_0^i: the upper and lower branches correspond respectively to time interfaces with a π-shift and without. Each branch is well fitted by a line which intersect at $a_0^f = 0$. This allows one to measure with a high precision the effective damping rate of the bath. We obtain in the present case $\nu_{\mathrm{eff}} = 8.3 \cdot 10^{-6}\ \mathrm{m^2.s^{-1}}$. This damping value is higher than the usual bulk viscosity owing to additional damping of the side walls of the cavity. This value can be used to compute the theoretical predictions from the damped Mathieu equation (see Fig. 3d and 4) showing a very good agreement with the experimental results without fitting parameters.

Discussion. – It is interesting to discuss the analogy between the temporal π-shift defects in time crystals and their spatial counterparts. Neglecting a possible saturation effect, both cases lead to waves decaying exponentially away from the interface and both show that the energy is confined to the defect. However, the origin of these localized excitations is different. In the case of spatial edge modes, the interface sets the boundary conditions which fully defines the existence of a localized topological edge mode. For time defects, however, causality implies that the growing wave mode excited prior to the time interface does not result from the interface itself. This latter is not a boundary condition involved in the existence of the waves for the previous times. The wave is a solution of the first time crystal only, associated to the Faraday instability in the present case. As a consequence, its amplitude at the time of the interface depends only on the size and excitation amplitude of the first crystal with a possible saturation due to non-linear effects. Such a growing mode is never observed in spatial crystals because of energy conservation. Energy band gaps are always forbidden gaps since the decaying solution is the only permitted one. There is no such energy considerations in time crystal and the growing mode can be observed. Consequently what could appear as a localized time edge mode should rather be considered as a permutation from a growing to a decaying crystal bulk mode in the k-gap, induced by the π-shift defect. However, such time defects provide us with a unique way to probe these bulk modes and probe the entire curve of Floquet exponents, including the usually hidden overdamped modes.

The vertical parametric excitation of a bath can be interpreted as a (degenerate) parametric amplifier of surface waves. When the Faraday instability threshold is reached, the amplifier goes into self-oscillation and the waves produced can be considered as modes of the degenerate parametric oscillator. This type of oscillators, which is also found in optics [33,34] and mechanics[35], produces so-called squeezed states which are characterized by the presence of unequal fluctuations following the two components in quadrature. Thus, since temporal defects enable probing the gains and attenuations of the two quadrature modes, they could also potentially be used to characterize the fluctuations occurring on each quadrature components of the squeezed states and be generalized to other types of systems.

***

The authors are grateful to Sander Wildeman for insightful discussions and help in the experiments. We thank the support of AXA research fund and the French National Research Agency LABEX WIFI (Laboratory of Excellence ANR-10-LABX-24).

REFERENCES

[1] SHAPERE A. and WILCZEK F., *Phys. Rev. Lett.,* **109** (2012) 160402.
[2] WILCZEK F., *Phys. Rev. Lett.,* **111** (2013) 1–8.
[3] SACHA K. and ZAKRZEWSKI J., *Rep. Prog. Phys.,* **81** (2017) 016401.
[4] ELSE D. V., BAUER B. and NAYAK C., *Phys. Rev. Lett.,* **117** (2016) 090402.
[5] YAO N. Y., POTTER A. C., POTIRNICHE I.-D. and VISHWANATH A., *Phys. Rev. Lett.,* **030401** (2017) 1–6.
[6] SACHA K., *Phys. Rev. A,* **91** (2015) 033617.
[7] KHEMANI V., LAZARIDES A., MOESSNER R. and SONDHI S. L., *Phys. Rev. Lett.,* **116** (2016) 250401.
[8] ZHANG J., HESS P. W., KYPRIANIDIS A., BECKER P., LEE A., SMITH J., PAGANO G., POTIRNICHE I.-D., POTTER A. C., VISHWANATH A., YAO N. Y. and MONROE C., *Nature*, **543** (2016) 217–220.
[9] PAL S., NISHAD N., MAHESH T. S. and SREEJITH G. J., *Phys. Rev. Lett.,* **120** (2018) 180602.
[10] HUANG B., WU Y.-H. and LIU W. V., *Phys. Rev. Lett.,* **120** (2018) 110603.
[11] GONG Z., HAMAZAKI R. and UEDA M., *Phys. Rev. Lett.,* **120** (2018) 040404.
[12] CHOI S., CHOI J., LANDIG R., KUCSKO G., ZHOU H., ISOYA J., JELEZKO F., ONODA S., SUMIYA H., KHEMANI V., KEYSERLINGK C. VON, YAO N. Y., DEMLER E. and LUKIN M. D., *Nature,* **543** (2017) 221–5.
[13] ROVNY J., BLUM R. L. and BARRETT S. E., *Phys. Rev. Lett.,* **120** (2018) 180603.
[14] SMITS J., LIAO L., STOOF H. T. C. and VAN DER STRATEN P., *Phys. Rev. Lett.* **121** (2018) 185301.
[15] HILL G. W., *Acta Math.,* **8** (1886) 1–36.
[16] STOLEN R. and BJORKHOLM J., *IEEE Journal of Quantum Electronics,* **18** (1982) 1062–72.
[17] MELDE F., *Annalen der Physik,* **187** (1860) 513–37.
[18] TURNER K. L., MILLER S. A., HARTWELL P. G., MACDONALD N. C., STROGATZ S. H. and ADAMS S. G., *Nature,* **396** (1998) 149–52.
[19] FARADAY M., *Philosophical Transactions of the Royal Society of London,* **121** (1831) 299–340.
[20] GIERGIEL K., MIROSZEWSKI A. and SACHA K., *Phys. Rev. Lett.,* **120** (2018) 140401.
[21] MIERZEJEWSKI M., GIERGIEL K. and SACHA K., *Phys. Rev. B,* **96** (2017) 140201.
[22] SACHA K. and DELANDE D., *Phys. Rev. A,* **94** (2016) 023633.
[23] AUTTI S., ELTSOV V. B. and VOLOVIK G. E., *Phys. Rev. Lett.,* **120** (2018) 215301.
[24] GIERGIEL K., DAUPHIN A., LEWENSTEIN M., ZAKRZEWSKI J. and SACHA K., *New J. Phys.,* **21** (2019) 052003.
[25] LUSTIG E., SHARABI Y. and SEGEV M., *Optica,* **5** (2018) 1390–5.
[26] WEIMANN S., KREMER M., PLOTNIK Y., LUMER Y., NOLTE S., MAKRIS K. G., SEGEV M., RECHTSMAN M. C. and SZAMEIT A., *Nature Mater,* **16** (2017) 433–8.
[27] DOUADY S., *J. Fluid Mech.,* **221** (1990) 383–409.
[28] BENJAMIN T. B. and URSELL F. J., *Proc. R. Soc. Lond. A,* **225** (1954) 505–15.
[29] BACOT V., DUREY G., EDDI A., FINK M. and FORT E., *PNAS,* **116** (2019) 8809–14.
[30] BACOT V., LABOUSSE M., EDDI A., FINK M. and FORT E., *Nature Physics,* **12** (2016) 972–977.
[31] KUMAR K. and TUCKERMAN L. S., *Journal of Fluid Mechanics,* **279** (1994) 49.
[32] XIAO Y., MAYWAR D. N. and AGRAWAL G. P., *Optics Lett.,* **39** (2014) 574.
[33] MILBURN G. and WALLS D. F., *Optics Communications,* **39** (1981) 401-404.
[34] COLLETT M. J. and GARDINER C. W., *Phys. Rev. A,* **30** (1984) 1386.
[35] RUGAR D. and GRÜTTER P., *Phys. Rev. Lett.,* **67** (1991) 699–702.